

NEW SCALING LAWS FOR SPACECRAFT DISCHARGE PULSES

A. R. Frederickson, Arthur.R.Frederickson@jpl.nasa.gov, 818-354-2105
California Institute of Technology Jet Propulsion Laboratory
Pasadena, CA 91109, USA

ABSTRACT

The electrostatic discharge pulse waveform, current as a function of time, was investigated as many parameters were varied. Electron beams from 5 keV to 1.5 MeV and beam current densities from 1 pA/cm² to 2 nA/cm² were used to charge insulating samples. FR4 circuit boards, electrical connectors, Duroid boards, space-rated Teflon-insulated wiring, Kapton wiring, and epoxy fiberglass were irradiated, and the resulting pulses were recorded. The old scaling laws were found to result from the condition of very high static electric field inside the insulator, fields beyond those expected in space service. At realistic internal static field strength, the pulse amplitude is much less than that predicted by the old scaling laws. For reasonable fields, the pulses do not clearly scale with sample area, and instead, become constant at areas larger than a few square centimeters. Additionally, the geometry of the electric field in the vacuum also controls the pulse amplitude. A scaling law for pulse event rate now appears obtainable. A scaling law for the voltage and energy imparted to any load resistance is now available. Pulse rate and amplitude both increase with increasing internal electric field. Usually, small electrodes receive only a small part of the pulsed current, but under some conditions all of the discharge current will go to a small electrode. A new conceptual framework has evolved such that it may now be possible to measure the static field strength and radiation-charging rate inside the insulator material by measuring the pulse rate.

INTRODUCTION

Existing scaling laws for discharge pulses were developed nearly twenty years ago and are based on an extended set of laboratory test results [1], repeated by a large number of researchers, but all for similar conditions. In those tests, samples were exposed typically to 20 keV electron beams of fairly high intensity. A few cases used mixed spectra of 20 keV electrons and higher energy electrons. The sample thicknesses were often of the order 100 micrometers or less. The samples were planar with only one grounded metalization covering the rear surface. The resulting pulses were consistent enough that scaling laws could be developed. Although those scaling laws appeared to be complex, our research suggests that they were the result of a simple process whereby a burst of gas developed a gas discharge into the vacuum space. The gas discharge proceeded to discharge the surface voltage on the insulator, and the meter current registered the current in the gas. There was ample gas to discharge most of the surface voltage over all of the sample and therefore the area scaling law was discovered. The current was controlled by the avalanche process in the gas and thus the pulse height and time duration scaling laws were discovered.

Recent extended tests under the NASA-MSFC SEE Program indicate that the original scaling laws are a subset of a more general set of scaling laws. In addition, different scaling laws are now indicated to describe how the pulse current partitions onto several sensitive nodes. Additionally, new scaling laws are now available for differing load resistors. It appears possible to develop scaling laws for pulse rate in the near future based upon electric field inside the insulator. Most importantly, the old scaling laws appear to be inapplicable in space conditions.

The earlier scaling laws were essentially a result of the following narrow conditions and the resulting consistent discharge phenomena. The dielectric samples were strongly stressed with order 10 kV across order 100 microns producing internal electric field of order 1E6 V/cm. The resulting pulses produced scaling laws which can succinctly be described as having triangular shape in I(t) with consistent slew rate, and always discharging more than half the original surface voltage over the entire sample area. In contrast, tests that provide more realistic space-like charging conditions produce a wide variety of scaling laws.

The new results find that the electric field inside the insulator is a critical term in controlling the pulse. In space, internal electric fields are closer to 1E5 V/cm. Once the potential differences on surfaces in the vacuum achieve a kilovolt or more, the field inside the insulator becomes a major controlling term. In addition, the divergence of the electric field in the vacuum becomes important [2]. Further, the arrangements of other surfaces and their impedance to ground strongly affects the current to any particular electrode. These effects are controlled by the evolution of the Townsend gas avalanche in the vacuum space after the partial discharge tree in the insulator injects a pulse of gas into the vacuum space. The evolution of gas is strongly dependent on the electric field in the insulator.

THE SPACECRAFT DISCHARGE PULSE

An equivalent circuit for the charging conditions is shown in Fig. 1. Here, the electron beam has charged the free surface of the insulator to some large negative voltage. The other surfaces are conductive and in contact with spacecraft

ground. Positive image charges flow in the conductors and appear on electrodes nearby the insulator in proportion to the capacitance between the trapped electron charges in the insulator and the electrode. Most of the images are in the metal attached to the insulator because this electrode has the most capacitance with respect to the region of stopped electrons.

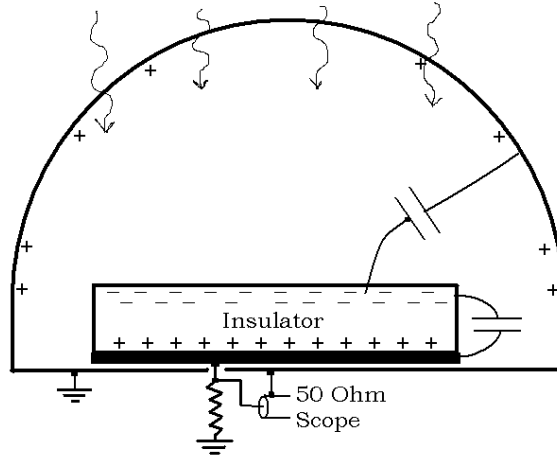


Figure 1. The Static Charging Condition. For every negative electron (-) stopped in the insulator there resides one positive image charge (+) somewhere in the surfaces of the metals near the insulator.

An equivalent circuit for the discharging conditions is shown in Fig. 2. The surface voltage, $V_s(t)$, drives current, I , through the plasma across the vacuum gap according to

$$I(t) = \frac{V_s(t)}{R(t)}. \quad (1)$$

V_s is a function of time, and is indicated to be 22 kV initially in Fig. 2, a common static charging level attained in ground tests using 30 kV electron beams.

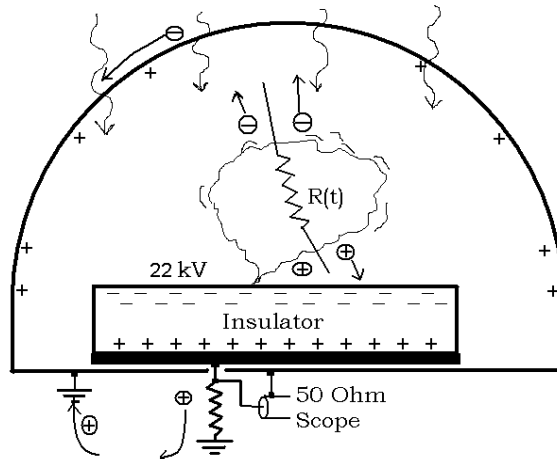


Figure 2. Charge Currents in Vacuum During the Pulse. Slightly ionized gas bursts from the insulator and a Townsend avalanche forms a conductive path in vacuum with time dependent resistance $R(t)$.

The resistance of the plasma, $R(t)$, depends instantaneously upon its charge density, neutral density, temperature and electric field in the vacuum. As current flows across the gap, positive image charges can move closer to the stopped electrons by flowing from each of the grounded electrodes and through the vacuum gap. Note the positive image charge current through the 50-ohm scope is specifically depicted in Fig. 2. If the surface potential, V_s , is known, the resistance at that instant can be determined from

$$R(t) = \frac{V_s(t)}{I(t)} - R_L, \quad (2)$$

where the oscilloscope (or other load) impedance is R_L . This equation assumes that the time resolution of the oscilloscope or other detector is slow compared to the time for light to transit the complete circuit path. We have assumed a quasi-static approximation for the plasma conduction.

Additionally, the plasmas applicable to our usual situation have impedances large compared to the load impedances typical of both the oscilloscope and the reactance of the electrodes. This fact allows us to use the simplified approximations of Eqs. 1-2.

PARAMETERS CONTROLLING THE SCALING LAWS

From the prior discussion it is clear that the scaling laws depend on the resistance of the plasma. Typical resistances exceed 1000 ohms in cases similar to real conditions in space. One can create very low plasma impedances, even 100 ohms or less, by irradiating the sample to very high internal electric fields, and thereby produce a dense low-impedance plasma burst. The old scaling laws were developed under conditions where relatively dense low-impedance plasmas were produced.

A few experimental examples of the phenomena and related parameters are presented. Nine scaling laws are deduced based on the experimental phenomena. Other scaling laws have also been deduced, but space limitations preclude their discussion.

EXPERIMENTS EXHIBITING NINE SCALING LAWS

I. Electric Field in the Vacuum.

The first experiment investigates the effect of varying only the electric field in the vacuum. This is done by using a constant electron beam on one sample while varying the distance through the vacuum gap from the sample surface to ground. For example, a planar sample with -10 kV on its surface, and spaced 10 cm from a coplanar ground plane will have an electric field of $10\text{kV}/10\text{cm} = 1 \text{ kV/cm}$ in the vacuum.

The details of this experiment are reported in [2], and mentioned in another paper at this conference. Briefly we compare the pulses from a planar 7.6 cm wide FR4 circuit board sample covered by a planar grounded-grid spaced 2.5 cm from it with the pulses from the same sample spaced roughly 70 cm from the large vacuum chamber grounded walls. In both tests the sample is charged to perhaps -20 to -25 kV by the 30 kV electron beam. The results are shown in Table 1.

It is clear from Table 1 that the strength of the vacuum electric field is not as critical as the form of the electric field. As discussed in [2] the divergence of the field seems to hold the neutral gas molecules near the sample for longer time allowing them to become involved in the Townsend avalanche. Without the field-divergence the neutral gas molecules more readily escape to the chamber walls without becoming ionized.

Table 1. Plasma Resistance vs. Electric Field.

Arrangement	Peak Current (Amps)	Initial Vacuum Field, Geometry	R(t) at Peak Current, ohms
Planar Grid	5.8	9 kV/cm planar	3000
Fully Open sphere	25.0	2 kV/cm spherically divergent	500

From this test we obtain a scaling factor: Divergent electric field in the vacuum space enhances the pulsed current amplitude relative to planar field of the same field strength.

II. Confinement of Discharge Gas

The second experiment investigates the effect of varying only the confinement of gas near the sample. This is done by varying the optical density of a grounded grid suspended 2.5 cm above the sample. One grid is 90% open thus allowing

gas to easily escape the region of high electric field in the vacuum. The other grid is similarly situated but only 32% open thereby significantly impeding the escape of gas molecules.

The details of this experiment are reported in [2], and mentioned in another paper at this conference. Briefly we compare the pulses from a planar 7.6 cm wide FR4 circuit board sample covered by the two planar grounded-grids.. In both tests the sample is charged to perhaps —20 to -25 kV by the 30 kV electron beam. The results are shown in Table 2.

From this test we obtain another scaling factor: Confining the movement of neutral gas within the electric field region enhances the conductance of the discharge.

Table 2. Plasma Resistance vs. Grid Openness

Grid Openness	Peak Current (Amps)	Initial Vacuum Field kV/cm	R(t) at Peak Current, ohms
90%	5.8	9	3000
32%	20.7	9	800

III. High Electric Field Inside the Insulator

The third scaling law is obtained by comparing the results in [1] with the results in [3]. In both cases the samples were thin and highly charged creating large internal field in the dielectric, $>2E6$ V/cm. With small samples [1], the field in much of the chamber is spherically divergent. With large samples [3], the field is nearly parallel. In these tests the samples were substantially discharged in each pulse. The old scaling laws were equivalent to the occurrence of the samples being substantially discharged in every pulse. Thus another scaling law is a dependence on internal electric field: The original scaling laws still hold for both planar geometry and divergent geometry when the insulator has internal fields in excess of $2E6$ V/cm.

IV Pulse Rate

FR4 circuit board, four samples of each thickness, was tested at 30 keV beam energy with three thicknesses: 3.17 mm, 1.59 mm and approximately 0.79 mm. First they were radiated for two days until a stable rate of pulsing developed. The data was taken in subsequent irradiations. The two thicker boards were irradiated at 0.5 nA/cm², but the thinnest board was irradiated at 0.1 nA/cm² in order to keep the pulsing slow enough for the scope and data-compiling computer to keep up with it.

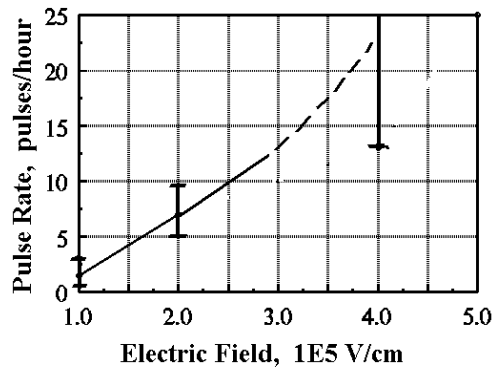


Figure 3. Pulse rate by 30 keV electrons on FR4 Circuit Board as a function of internal electric field. All three points used 30 keV electrons, so the beam energy appears to be unimportant.

Knowing the beam energy one may estimate the electric field strength in the sample. The results for the three thickness are provided in Fig. 3. The curve is dashed because the dead-time effect at the high beam energy makes it difficult to evaluate both the actual pulse rate and the electric field. It is clear that the pulse rate depends on electric field.

A cable bundle test was performed at 0.5 nanoamperes per square centimeter at electron beam energies from 10 keV to 30 keV. With cables it is difficult to estimate the internal electric field and the surface voltage because the geometry is so complex. It suffices to know that in this energy range the insulation is not penetrated, and the surface potential and internal electric fields scale approximately with electron beam energy. Being cylindrical and irradiated by a plane parallel beam, various parts of the insulation are at various voltages and electric field strengths. The following graph of pulse rate and pulse peak amplitude with respect to electron beam energy indicates that rate and amplitude both scale with electric field strength. This relationship has been found to be true in all data sets where it is possible to analyze the data in this manner.

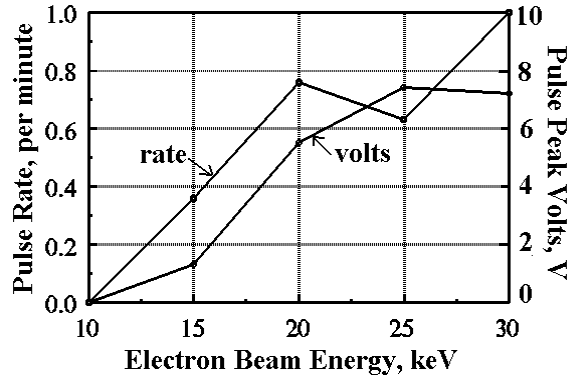


Figure 4. Dependence of pulse rate and pulse amplitude on beam energy. The internal electric field scales with beam energy, and is the actual cause of increasing pulse rate and amplitude.

For comparison to other tests it helps to know how much material was irradiated. The bundle was about 1.2 cm diameter, and 60 cm long. Only the outer jacket was exposed to radiation. No radiation impacted the wires at the end of the cable, nor penetrated the jacket.

Thus we have a scaling law for pulse rate. The pulse rate is roughly proportional to the internal dielectric field-strength raised to a (unknown) positive power. It goes to zero somewhat below $1E5$ V/cm.

V. Pulse Amplitude.

Figure 4 indicates the dependence of pulse peak amplitude on internal electric field. The total charge as well as the total energy into the load resistor showed similar dependence. All samples showed similar tendency. Thus we have the fifth scaling law. The quantity of gas injected into vacuum, and therefore its ability to discharge surface area, decreases strongly as internal electric field decreases and goes to zero somewhat below $1E5$ V/cm. The peak current, total charge, and pulse energy similarly decrease.

VI. Relation Between Pulse Rate and Pulse Amplitude.

Combining IV and V one determines that, on a particular sample, decreasing pulse rates are associated with decreasing charge and energy in the associated pulses.

VII, VIII. Pulsed Current Distribution Amongst Several Electrodes.

Several tests were performed to determine the fraction of current distributed to individual wires or traces. All results were similar in that the smaller traces shared smaller currents. The plasma current did not connect to a single element across the vacuum. The following test is interesting.

First consider the circuit board in Fig. 5. Discharges were generated by electron radiation from 10 keV up to 1 MeV. The results of interest here did not depend on the beam energy. (Of course pulse amplitude, pulse frequency and surface voltage did depend on internal field and thus on beam energy.) The boards were approximately 7 cm x 7 cm in size, and both Duroid and FR4 boards were tested. The observed phenomena are adequately explained by the gas discharge concept.

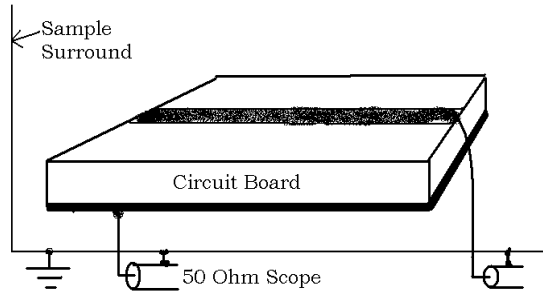


Figure 5. Experiment to measure current collected by a small electrode.

The pulses on the rear electrode were relatively large and positive because as the surface of the insulator discharged, the positive image charge in the rear electrode went to ground through the scope.

The pulses on the strip of copper at the front of the board, however, were always relatively small, sometimes only positive, and often bipolar. A small amount of positive image charge also resides on the copper strip prior to each discharge. Sometimes the gas of the discharge did not connect to the copper strip, and in this case only a small positive pulse would be seen from the copper strip. But other times the gas would connect to the copper strip and turn the initially positive pulse rapidly into a negative pulse as the negative potential of the insulator surface drove current through the gas onto the copper strip. The total charge in the negative-going pulses was also relatively small, but often larger than the charge in the positive-only pulses.

The charge in the rear electrode pulse was always larger than the charge in the copper strip pulse. Thus, it appears that the plasma spreads out widely in the chamber and delivers the discharge current over a wide region in the chamber, mostly to chamber walls. Thus, when it is not constrained the gas avalanche distributes current widely.

Other insulated surfaces will be either further-charged or partially discharged depending on their potential relative to the potential of the avalanching gas and the initial discharging surface. Thus, some current will be delivered (capacitively) to electrodes that underlay those other insulated surfaces.

The gas may be constrained to flow to ground via a tortuous path by other insulators. Figure 6 describes how a (25 micron) Kapton blanket was used to investigate the effect. The Kapton was not metal coated. Electron beams from 100 keV to 1 MeV were used to penetrate the Kapton and bombard the circuit boards. The figure is an approximate cross sectional scale drawing of the test apparatus.

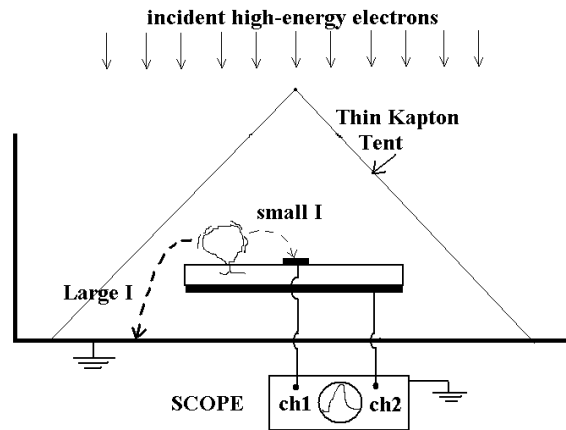


Figure 6. Experiment to demonstrate that discharge current goes around barriers.

The pulsing results were not significantly changed relative to the results discussed above for the unconstrained gas discharges. The majority of the discharge current flowed through the gas to the grounded chamber walls behind the samples as shown in Fig. 6 by the words Large I. Only small discharge current went to the copper strip on the front of the boards, as in the prior experiment.

The gas discharge can be constrained so that it may discharge the insulator surface only through the copper strip. Figure 7 describes the test geometry. The 25 micron Kapton blanket constrains the gas so that it can not pass across the vacuum to the chamber walls. A small hole was punched into the Kapton for vacuum purposes. Electron beams from 100 keV to 1 MeV were used to penetrate the Kapton. The samples were the same samples as in the prior tests.

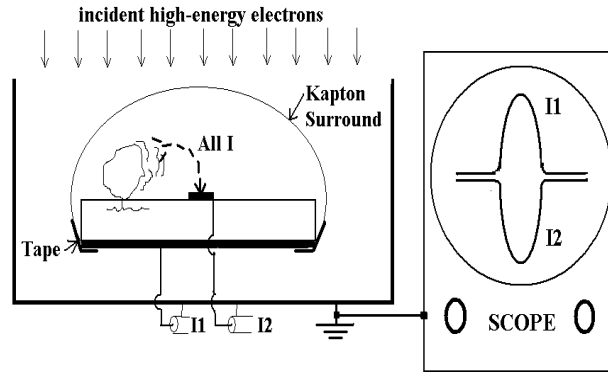


Figure 7. Experiment that proves that with constrained gas, all current may concentrate on a small electrode.

Because of the Kapton barrier, the gas is not able to carry current to any grounded object except for the copper strip. Thus, in this experiment every one of the pulses had the copper strip current equal and opposite to the rear electrode current. The oscilloscope traces were more complex than shown in this drawing. The traces were large like those on the rear electrode without the Kapton barrier. No matter what the pulse shape, I1 and I2 were nearly perfect mirror images of each other.

Based on the results of the tests in Figs. 6,7, and many other tests, we have two more scaling laws. 7. If the ionized gas current flows to more than one electrode, because the gas is diffuse it will roughly spread to electrodes proportional to their area, except when

.VIII. Divergent electric fields and material surfaces modify the flow of the gaseous discharge current and must be considered in order to estimate its amplitude at a particular electrode.

IX. Pulse Amplitude impressed on other load resistors

To understand what happens to resistors not at 50 ohms, refer to figure 2. The sample surface, perhaps at 22 kV, drives current through the plasma to the grounded walls of the chamber. If at this time one ampere flows then the resistance of the plasma must be $22,000 - 50 = 21950$ ohms at this instant. The instantaneous power in the load is $I^2R = 50$ watts.

Consider the load resistor, normally the 50 ohm scope. Suppose it were changed to 1000 ohms. How would the pulse amplitude change at the same instant? The total impedance would be 23,000 ohms, and therefore the current would be $22,000/23,000 = 0.957$ Amperes. The instantaneous power in this load resistor would be $I^2R = 915$ watts. For the case of load resistor impedance-matched to the source (22 k-ohms) the instantaneous power would be $I^2R = 5.5$ kW, and the instantaneous voltage would be 11 kV.

An experiment was performed with one sample using two load resistors, 50 ohms and 1000 ohms. This sample typically created 1-ampere pulses with 20 to 35 kV electron radiation. The pulsed current waveforms were not measurably attenuated in the 1000-ohm case relative to the 50-ohm case. The 1000-ohm load experienced peak voltages 20-times larger than did the 50-ohm load, and total energy dissipation 20-times larger than experienced by the 50-ohm load. With this information one may scale the results from one load resistance to another. One determines the pulsed voltage, $V(t)$, on the load resistor, R_L , such that the current, $I(t)$, through the load resistor in series with the impedance of the gas discharge, $R_G(t)$, equals the time dependent surface voltage, $V_S(t)$. Thus, $V(t)=I(t) \times R_L$ where $V_S(t)=I(t) \times [R_L + R_G(t)]$. R_G can range from 100 ohms for samples with large internal electric field ($>2E6$ V/cm) to 100 k-ohms for samples with small internal electric field ($1E5$ V/cm).

SUMMARY OF NEW SCALING LAWS

I. Divergent electric field in the vacuum space enhances the pulsed current amplitude relative to planar field of the same field strength. The quantity of enhancement is an unknown function of the gas density and the molecules comprising the gas.

II. Confining the movement of neutral gas within the electric field region enhances the conductance of the discharge.

III. The original scaling laws still hold for both planar geometry and divergent geometry when the insulator has internal fields in excess of $2E6$ V/cm. This means that for typical spacecraft structures, the entire area of the charged insulator will be substantially discharged by at least half when the initial surface voltage exceeds 1 kV.

IV. The pulse rate is roughly proportional to the field-strength internal to the insulator raised to a (unknown) positive power. It goes to zero somewhat below $1E5$ V/cm.

V. The quantity of gas injected, and therefore its ability to discharge surface area, decreases strongly as internal electric field decreases and goes to zero somewhat below $1E5$ V/cm. The peak current, total charge, and pulse energy similarly decrease.

VI. On a particular sample, decreasing pulse rates are associated with decreasing charge and energy in the respective pulses.

VII. If the ionized gas current flows to more than one electrode, because the gas is diffuse it will roughly spread to electrodes proportional to their area, except when

VIII. Divergent electric fields and material surfaces modify the flow of the gaseous discharge current and must be considered in order to estimate its amplitude.

IX. One determines the pulsed voltage, $V(t)$, on the load resistor, RL , such that the current, $I(t)$, through the load resistor in series with the impedance of the gas discharge, $RG(t)$, equals the time dependent surface voltage, $VS(t)$. Thus, $V(t)=I(t) \times RL$ where $VS(t)=I(t) \times [RL + RG(t)]$. RG can range from 100 ohms for samples with large internal electric field ($>2E6$ V/cm) to 100 k-ohms for samples with small internal electric field ($1E5$ V/cm).

REFERENCES

1. K. G. Balmain and G. R. Dubois, Surface Discharges on Teflon, Mylar and Kapton, IEEE Trans. Nuc. Sci. 26, 5146-51. Dec. 1979.
2. A. R. Frederickson, C. E. Benson and E. M. Cooke, Gaseous Discharge Plasmas Produced by High-energy Electron-irradiated Insulators for Spacecraft, IEEE Trans. Plasma Science 28, 2037-47, Dec. 2000.
3. T. M. Flanagan, R. Denson, C. E. Mallon, M. J. Treadaway, and E. P. Wenaas, Effect of Laboratory Simulation Parameters on Spacecraft Dielectric Discharges, IEEE Trans. Nuc. Sci. 26, 5134-40, Dec. 1979. This work and others by the same authors are complementary to Ref. 1.

keywords: spacecraft charging, spacecraft discharge, scaling laws, discharge pulse, dielectric discharge, partial discharge, radiation, high-energy electrons.

The research described in this paper was carried out by the Jet Propulsion Laboratory, California Institute of Technology, under a contract with the National Aeronautics and Space Administration and the NASA SEE Space Environmental Effects Program.